

# Mechanisms of heavy metal sorption on alkaline clays from Tundulu in Malawi as determined by EXAFS

S.M.I. Sajidu<sup>a,\*</sup>, I. Persson<sup>b</sup>, W.R.L. Masamba<sup>c</sup>, E.M.T. Henry<sup>✝</sup>

<sup>a</sup> Chemistry Department, University of Malawi, P.O. Box 280, Zomba, Malawi

<sup>b</sup> Department of Chemistry, Swedish University of Agricultural Sciences, Box 7015, 75007 Uppsala, Sweden

<sup>c</sup> Harry Oppenheimer Okavango Research Centre, University of Botswana, P/Bag 285, Maun, Botswana

Received 28 August 2007; received in revised form 24 January 2008; accepted 25 January 2008

Available online 6 February 2008

## Abstract

Chromium(III), copper(II), zinc(II), cadmium(II), mercury(II) and lead(II) cations are among the most common heavy metal pollutants in industrial waste waters. In our continued work on cost effective wastewater heavy metal removal agents and methods using local material, this study examines the interactions of chromium(III), copper(II), zinc(II), cadmium(II), mercury(II) and lead(II) cations with natural mixed clay minerals from Tundulu in Malawi using extended X-ray absorption fine structure (EXAFS) spectroscopy. The mixed clays were previously characterised and found to contain illite, low ordered kaolinite, mixed layer minerals and the non-clay mineral carbonate fluoroapatite with a mean  $pH_{PZC}$  of 9.63. The EXAFS analyses provided qualitative evidence that oxygen atoms occupy the first coordination shells in all the studied central atoms. The metal species on the clay mineral surfaces seem to be adsorbates and/or precipitates of hydrolysis products. Chromium(III) forms a polynuclear hydrolysis complex on the mineral surface with Cr–O bond and Cr···Cr distances of 2.00 and 3.03 Å, respectively, which is indicative of a chain structure with edge sharing  $CrO_6$  octahedra. Copper(II) is bound to phosphate groups on the surface at low pH and has a first shell of coordinated oxygen atoms with Jahn–Teller distortion as revealed by different Cu–O bonds of 1.96 Å for the equatorial ones, at 2.30 and 2.65 Å for the axial oxygens, and a Cu–P distance at 3.29 Å is distinguished as well. Upon treatment at neutral pH copper(I) oxide seems to be the main precipitation product on the clay surface. At neutral pH zinc(II) forms also polynuclear hydrolysis complexes with Zn–O bond and Zn···Zn distances of 2.01 and 3.11 Å, respectively, which shows the presence of edge sharing  $ZnO_4$  tetrahedra. Cadmium(II) is adsorbed to the clay surfaces as a six-coordinated  $CdO_6$  complex in octahedral fashion, but it is not possible to distinguish if cadmium is hydrated or partly hydrolysed. Mercury(II) is present as linear O–Hg–O units but without any observable Hg···Hg distance at high pH showing that mercury(II) is hydrolysed but not present as mercury(II) oxide. At low pH, linear O–Hg–Hg–O units are present showing that mercury(II) is reduced to mercury(I). No precise chemical environment around the lead(II) could be obtained for the lead(II) treated clays due to formation of different hydrolysis structures with multiple coordination numbers by lead(II) salts on the mixed clays.

© 2008 Elsevier B.V. All rights reserved.

**Keywords:** Heavy metal; Tundulu mixed clay;  $pH_{PZC}$ ; EXAFS; Polynuclear hydrolysis complex

## 1. Introduction

There have been studies on the removal of heavy metals from water and wastewater including chemical precipitation, physical treatment such as ion exchange, solvent extraction and

adsorption. However, due to high maintenance costs and chemical importation using scarce convertible foreign currency, these methods are unsustainable in developing countries. Recently, natural materials which are good sorbents and inexpensive have received much attention in sorption of heavy metals from contaminated water. Clay minerals such as montmorillonite and vermiculite [1–3], allophane [4], kaolinite [5], bentonite [6,7] and illite [8] are among the natural materials which have been investigated as heavy metal sorbents owing to their high cationic exchange capacity and negative charges due to isomorphous substitution in their structures. Our work on the removal of heavy metals from contaminated water using locally available cost

\* Corresponding author. Tel.: +265 1 524 222; fax: +265 1 524 046.

E-mail addresses: [sajidu@chanco.unima.mw](mailto:sajidu@chanco.unima.mw), [ssajidu@yahoo.co.uk](mailto:ssajidu@yahoo.co.uk) (S.M.I. Sajidu), [Ingmar.Persson@kemi.slu.se](mailto:Ingmar.Persson@kemi.slu.se) (I. Persson), [wmasamba@orc.ub.edu](mailto:wmasamba@orc.ub.edu) (W.R.L. Masamba).

✝ Deceased.

effective materials is focused on clays and *Moringa* seed extracts [9–11]. The present study, in continuation of our reported work in Ref. [10], focuses at the interactions of heavy metals, present as single solutes in aqueous system, with the surfaces of natural mixed clay minerals obtained from the Tundulu area in Malawi using extended X-ray absorption fine structure (EXAFS) spectroscopy. The Tundulu natural clays are mixtures of illite, low ordered kaolinite, carbonate fluoroapatite with a possibility of mica, smectite or vermiculite mixed layers as well [10]. Their mean  $\text{pH}_{\text{PZC}}$  and cation exchange capacity are 9.63 and 19.7  $\text{cmol}_c/\text{kg}$ , respectively. Our previous studies have demonstrated the successful lab scale application of the Tundulu mixed clays for heavy metal removal from aqueous solution [10]. The sorption of chromium(III), copper(II), zinc(II), cadmium(II), mercury(II) and lead(II) ions on the mixed clays was characterised as a function of pH. It was found that due to the alkaline nature of the clays complete removal of these cations would be achieved without addition of a base or acid for different initial concentrations of the metals at different clay doses.

In this work, EXAFS was used to characterize the sorbed chromium(III), copper(II), zinc(II), cadmium(III), mercury(II) and lead(II) ions on the clay surfaces. The main advantages of EXAFS are that the nearest neighbour distances around the absorbing element are observed and all states of aggregation can be studied with high precision in the distances even in very dilute samples with metals sorbed on mineral or clay surfaces. An example on the use of this technique is provided by the interaction of cadmium(II) solution with thiol-functionalised 2:1 clay minerals where cadmium was found to give monomer complexes or CdO molecules on the surfaces or interlayers of the untreated clay minerals with Cd–O distance of 2.24 Å while Cd–S clusters were formed on the thiol-functionalised clay minerals [3]. However earlier EXAFS studies about cadmium sorption on montmorillonite revealed outer sphere complex formation at lower pH and surface precipitate at higher pH as  $\text{Cd}_5(\text{OH})_{18}(\text{NO}_3)(\text{H}_2\text{O})$ -like structures [12]. In the study of mercury(II) interaction with goethite surface [13] the distance between the adsorbed mercury and the two closest oxygen atoms in the mineral was found to be 2.04 Å and the distance between Hg and Fe was 3.28 Å giving  $\angle \text{Fe–O–Hg} = 108^\circ$ . Structural studies on effects of chloride and sulphate on the interactions between Hg and Fe- and Al-(hydr)oxides using EXAFS were carried out by Kim et al. [14]. Mercury adsorption on montmorillonite and vermiculite has been found to result in formation of montroydite-like structures characterised by EXAFS [2]. Investigations on the local structural environment of chromium(III) sorbed on silica using EXAFS have been reported in Ref. [15]. Their results showed formation of monodentate chromium(III) surface complex on silica with Cr–Si distance of 3.39 Å for the sorbed chromium while formation of polynuclear chromium hydroxide octahedra was discerned on the surface. Zinc uptake on hydroxyapatite has been studied using EXAFS technique and the results have indicated precipitation of  $\text{Zn}_3(\text{PO}_4)_2 \cdot 4\text{H}_2\text{O}$  as the dominating mechanism of zinc uptake [16].

Despite many works dealing with heavy metal adsorption properties of clay minerals, only very few of them have dealt

with the actual heavy metal interactions with the clay minerals. In continuation of our reported work on sorption of heavy metals on Tundulu natural alkaline clays, this study aimed at investigating the local structural environment of chromium(III), zinc(II), cadmium(II), mercury(II) and lead ions sorbed on the natural alkaline mixed clays.

## 2. Materials and methods

### 2.1. Samples

The clay samples were collected from the Geological Survey of Malawi and purified as described elsewhere [17,18]. Briefly, in order to remove carbonates, 100 g of raw mixed clay was dispersed in 100 ml 1.0  $\text{mol dm}^{-3}$  sodium acetate–acetic acid buffer (8.2 g sodium acetate and 6 g pure acetic acid per 100 ml of water, pH 4.8) and stirred from time to time for a few days until there was no more evolution of carbon dioxide bubbles (indicating presence of carbonates). The slurry was then centrifuged and dispersed in 270 ml citrate buffer (115 g (0.37 mol) sodium citrate dihydrate, 8.5 g (0.1 mol) sodium hydrogencarbonate and 70 g (1.2 mol) sodium chloride per litre) in order to remove iron oxides. pH was adjusted to 8.3 and 20 g of sodium dithionite was added. The slurry was stirred for 70 h, centrifuged and washed four times with a solution of 0.5  $\text{mol dm}^{-3}$  sodium chloride and 0.025  $\text{mol dm}^{-3}$  hydrochloric acid. The entire procedure was repeated once more. In order to remove organic matter, 500 ml of 0.1  $\text{mol dm}^{-3}$  sodium acetate solution and 170 ml of 30% (w/w) hydrogen peroxide solution were added to the slurry and the mixture was stirred for 10 h at 90 °C and then for 20 h at room temperature. The clay was then washed three times with 1  $\text{mol dm}^{-3}$  sodium chloride solution. Finally it was washed with distilled water to remove excess salt, dried and then ground to powder. Clay fractionation was done by mixing the powder with water and transferring the slurry to a cylinder (30 cm high). This was then diluted to a volume higher than 10 cm. The suspension was shaken to homogeneity and allowed to stand undisturbed for 8 h. Thereafter the clay suspension above 10 cm was siphoned to a bucket and concentrated by centrifugation and dried in air.

### 2.2. Metal sorption

A 20  $\text{mmol dm}^{-3}$  copper(II), zinc(II), cadmium(II), and lead(II) solutions were obtained from dissolution of analytical grade reagent  $\text{Cu}(\text{NO}_3)_2 \cdot \text{H}_2\text{O}$ ,  $\text{Zn}(\text{NO}_3)_2 \cdot 6\text{H}_2\text{O}$ ,  $\text{Cd}(\text{NO}_3)_2 \cdot 4\text{H}_2\text{O}$ , and  $\text{Pb}(\text{NO}_3)_2$  respectively in deionized water. A 20  $\text{mmol dm}^{-3}$  chromium(III) solution was prepared by dilution of a 1.4  $\text{mol dm}^{-3}$   $\text{Cr}(\text{ClO}_4)_3 \cdot 6\text{H}_2\text{O}$  stock solution (prepared from chromium(III) perchlorate hexahydrate,  $\text{Cr}(\text{ClO}_4)_3 \cdot 6\text{H}_2\text{O}$  in 1.0  $\text{mol dm}^{-3}$  hydrochloric acid). A 20  $\text{mmol dm}^{-3}$  aqueous mercury(II) trifluoromethanesulfonate solution was prepared by dissolving anhydrous  $\text{Hg}(\text{CF}_3\text{SO}_3)_2$  in deionized water at pH 2.0 adjusted by addition of nitric acid.

Twenty-five millilitres of the 20  $\text{mmol dm}^{-3}$  of the metal solution was added to 1.0 g of the clay and the pH was adjusted to 7.0 by dropwise addition of 1.0  $\text{mmol dm}^{-3}$  NaOH for the

suspensions treated with chromium(III), copper(II), zinc(II) mercury(II) and lead(II) whereas the clay suspension treated with cadmium(II) was adjusted to pH 9.0. The clay suspensions were stirred for 48 h at room temperature and then centrifuged to separate the rich adsorbed clay samples which were dried in air before the EXAFS measurements. Separate samples at low pH values were also prepared for the EXAFS measurements. The low pH values were adjusted to 3.2, 4.7, 6.2 and 2.2 for chromium(III), copper(II), zinc(II) and mercury(II), respectively.

### 2.3. EXAFS—data collection

Chromium, copper, zinc and cadmium K-edge spectra and mercury and lead L<sub>3</sub>-edge X-ray absorption spectra were collected at the bending magnet beam line 2–3 at the Stanford Synchrotron Radiation Laboratory (SSRL), Stanford, USA, which was operated at 3.0 GeV and a maximum current of 100 mA, and at beam-line I811, MAX-lab, Lund University, Sweden, which was operated at 1.5 GeV and a maximum current of 200 mA. Cadmium data for the low pH samples were not collected because the maximum beam energy at MAX-lab (20 keV) is lower than the cadmium K-edge absorption energy (26.711 keV). Data collection was performed in transmission and fluorescence mode simultaneously, except for cadmium where only transmission data were collected. The fluorescence measurements were performed with a Lytle detector with a suitable X-ray filter and with a very gentle flow of argon and/or krypton gas depending on energy. The EXAFS stations were equipped with a Si[2 2 0] (SSRL) or Si[1 1 1] (Max-lab) double crystal monochromator. In order to remove higher order harmonics, the beam intensity was detuned to 30, 50, 50, 80, 50 and 50% for chromium, copper, zinc, cadmium mercury and lead, respectively, at the end of the scans. Internal energy calibration was made with corresponding metal foil, and in case of mercury with boron nitride diluted mercury(II) chloride sample [19]. For each sample three to four scans were averaged. The treatment of the EXAFS data was carried out by means of the EXAFSPAK program package [20], using standard procedures for pre-edge subtraction and spline removal.

### 2.4. EXAFS—data analysis

The EXAFSPAK program package [20] was used for the data treatment. The EXAFS oscillations were obtained after performing standard procedures for pre-edge subtraction, and spline removal. The  $k^3$ -weighted model functions were calculated using ab initio calculated phase and amplitude parameters obtained by the FEFF7 program [21]. Input to the FEFF7 program was prepared by taking appropriate angles and distances for solid hexa-aquacadmium(II) perchlorate [22], diammonium hexa-aquachromium(III) pentafluoride [23], mercury(II) oxide [24], bisaquatetratrifluorosulfatomercury(II) [25], strontium tetrahydroxozincate hydrate, Sr[Zn(OH)<sub>4</sub>]<sub>2</sub>·H<sub>2</sub>O [26] and zinc(II) oxide [27].

The standard deviations given for the refined parameters in Table 1 are obtained from  $k^3$ -weighted least squares refinements

of the EXAFS function  $\chi(k)$ , and do not include systematic errors of the measurements. These statistical error estimates provide a measure of the precision of the results and allow reasonable comparisons, e.g. of the significance of relative shifts in the distances. However, the variations in the refined parameters, including the shift in the  $E_0$  value (for which  $k=0$ ), using different models and data ranges, indicate that the absolute accuracy of the distances given for the separate complexes is within  $\pm 0.01$ – $0.02$  Å for well-defined interactions. The “standard deviations” given in the text have been increased accordingly to include estimated additional effects of systematic errors.

## 3. Results

### 3.1. Chromium(III) treated clay samples

The non-sinusoidal shape of the EXAFS function at pH 7 shows the presence of at least two significant back-scatterer distances, Fig. 1. The FT shows light back-scatterer, certainly oxygen, at short distance, 2.00 Å, and a heavier back-scatterer, most probably chromium, at ca. 3.0 Å, and a smaller contribution at ca. 4.0 Å, multiple scattering within the expected CrO<sub>6</sub> core. These distances fit very well with the structure of hydrolysed chromium(III) complexes in aqueous solution. Two hydrolysis complexes have been identified in aqueous solution [Cr<sub>3</sub>(OH)<sub>4</sub>(H<sub>2</sub>O)<sub>10</sub>]<sup>5+</sup> present in aqueous chromium(III) solution with pH  $\approx$  3.5, and indefinite [Cr(OH)<sub>x</sub>-(OH)<sub>2</sub>]<sub>n</sub><sup>n(2x-3)+</sup> chains with double hydroxo bridges and each chromium also binds additionally two hydroxide ions/water molecules ful-

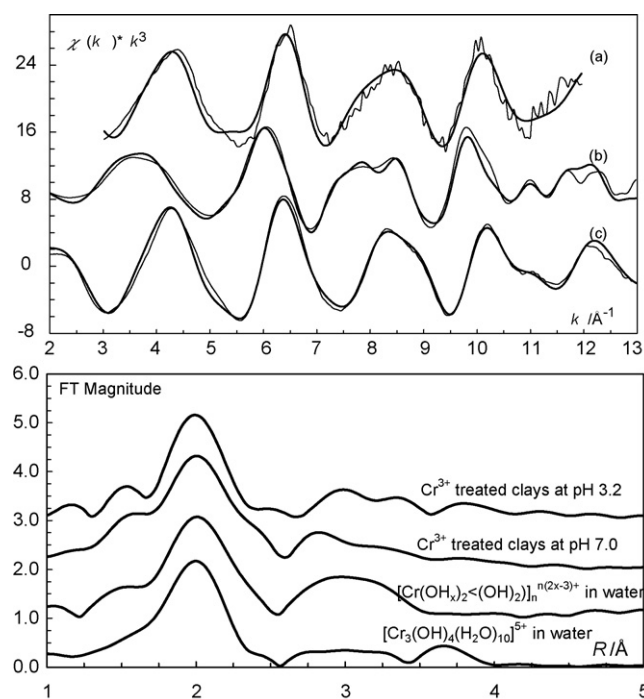


Fig. 1. Upper panel: (a)  $k^3$ -weighted Cr K-edge EXAFS  $\chi(k)$  spectra for Cr-clay samples treated at pH 7.0 (light line), (b) [Cr(OH)<sub>x</sub>-(OH)<sub>2</sub>]<sub>n</sub><sup>n(2x-3)+</sup> and (c) [Cr<sub>3</sub>(OH)<sub>4</sub>(H<sub>2</sub>O)<sub>10</sub>]<sup>5+</sup> compared with the theoretical signals (bold lines). Lower panel: phase shifted Fourier transforms of the EXAFS data.

Table 1  
Mean bond lengths (or distances),  $R$  (Å), Debye–Waller factors,  $\sigma^2$ , numbers of distances,  $N$ , around the metal ions sorbed on clay surfaces treated with dilute metal salt solutions at neutral and acidic pH as determined by EXAFS

Interaction	Treated at pH 7.0			Treated at pH 3.2		
	$N$	$R$ (Å)	$\sigma^2$ (Å <sup>2</sup> )	$N$	$R$ (Å)	$\sigma^2$ (Å <sup>2</sup> )
Cr–O	6	2.007 (3)	0.0021 (5)	6	1.958 (3)	0.0023 (4)
MS(CrO <sub>6</sub> )	3 × 6	3.99 (2)	0.008 (2)	3 × 6	3.94 (2)	0.008 (2)
Cr···Cr	1.67	3.013 (6)	0.0044 (7)	1	3.003 (5)	0.0050 (4)
Cr···Cr	0.33	3.59 (2)	0.0031	2	3.57 (2)	0.0069 (6)

Interaction	Treated at pH 7.0			Treated at pH 4.7		
	$N$	$R$ (Å)	$\sigma^2$ (Å <sup>2</sup> )	$N$	$R$ (Å)	$\sigma^2$ (Å <sup>2</sup> )
Cu–O	4	1.860 (3)	0.0043 (3)	4	1.955 (3)	0.0044 (4)
Cu–O				1	2.30 (2)	0.010 (3)
Cu–O	1			1	2.65 (1)	0.005 (2)
Cu–P	1			1	3.292 (6)	0.0045 (7)
MS(CuO <sub>4</sub> )	3 × 4	3.79	0.0128	3 × 4	4.01 (3)	0.009 (3)
Cu···Cu	1	3.350 (11)	0.0096 (12)			
Cu···Cu	4	4.243 (7)	0.0093 (7)			

Interaction	Treated at pH 7.0			Treated at pH 6.2		
	$N$	$R$ (Å)	$\sigma^2$ (Å <sup>2</sup> )	$N$	$R$ (Å)	$\sigma^2$ (Å <sup>2</sup> )
Zn–O	4	2.014 (8)	0.0055 (11)	4	2.012 (5)	0.0040 (6)
Zn···Zn	1	3.157 (8)	0.0070 (7)	1	3.149 (6)	0.0133 (6)
Zn···Zn	1	3.67 (2)	0.010 (1)	1	3.56 (2)	0.021 (2)

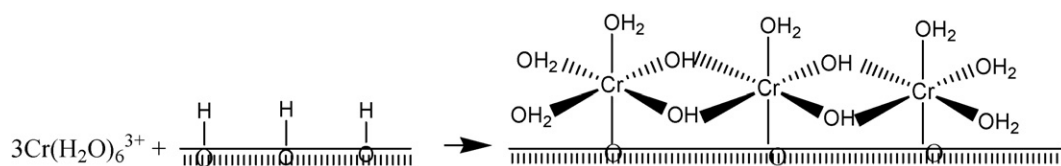
Interaction	Treated at pH 9.0		
	$N$	$R$ (Å)	$\sigma^2$ (Å <sup>2</sup> )
Cd–O	6	2.270 (5)	0.0082 (6)
MS(CdO <sub>6</sub> )	3 × 6	4.57 (1)	0.011 (1)

Interaction	Treated at pH 7.0			Treated at pH 2.2		
	$N$	$R$ (Å)	$\sigma^2$ (Å <sup>2</sup> )	$N$	$R$ (Å)	$\sigma^2$ (Å <sup>2</sup> )
Hg–O	2	2.054 (5)	0.0015 (5)	2	2.001 (4)	0.0026 (5)
Hg–Hg				1	2.514 (6)	0.0029 (5)
MS(HgO <sub>2</sub> )	2 × 2	4.13 (2)	0.003 (1)			

filling an octahedral configuration present in very alkaline aqueous solutions, pH > 14 [28]. It seems that both types of chromium(III) hydrolysis complexes are present on the clay surfaces with predominance of the indefinite chains as the contribution at 3.6 Å, typical of the trimer, is present but suppressed in comparison with the pure  $[\text{Cr}_3(\text{OH})_4(\text{H}_2\text{O})_{10}]^{5+}$  complex. The trimer predominates at lower pH (EXAFS plot not shown). Any presence of solid chromium(III) oxide on the clay surfaces can be ruled out as the Cr–O bond and Cr···Cr distance in  $\text{Cr}_2\text{O}_3$  are significantly shorter than the distances observed of the chromium(III) species in this study. The refined structure

parameters are given in Table 1, and the fit of the experimental EXAFS data, and the corresponding FTs, are given in Fig. 1. A possible interaction of the chromium(III) cations on the clays in the trimeric form is shown in Scheme 1. The proposed Scheme 1 and those in the subsequent sections are based on the EXAFS results. Long-range distances expected in well defined precipitations were not observed and the metals in most cases were in hydrolysed form. The proposed models (schemes) are therefore likely (but not any definite) and fit the observations made by EXAFS. There is certainly room for other alternatives in detailed models.



Scheme 1.



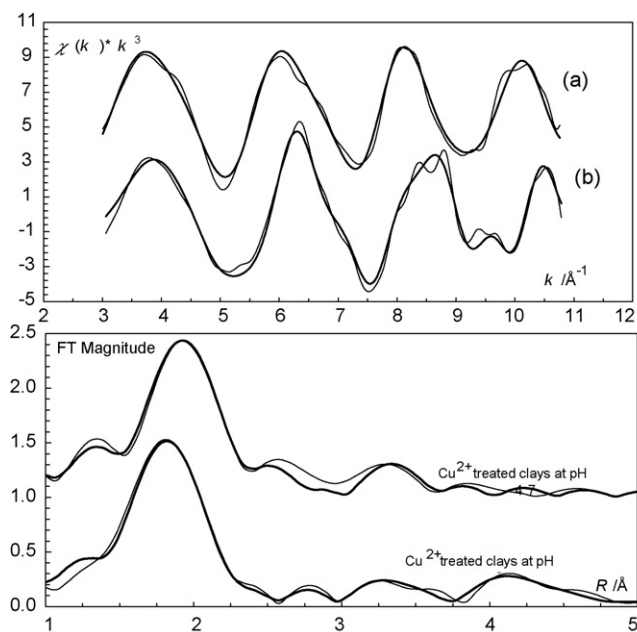
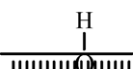
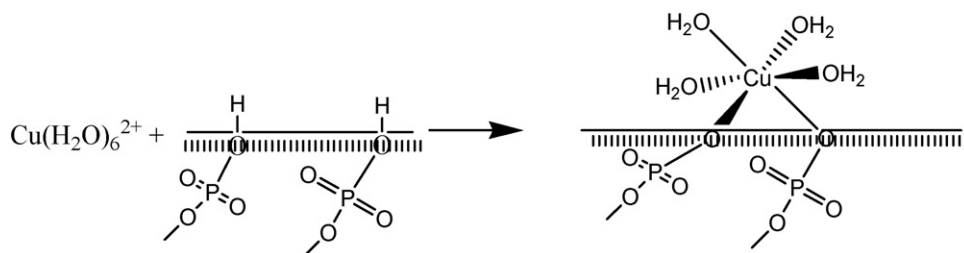


Fig. 2. Upper panel (a) and (b):  $k^3$ -weighted Cu K-edge EXAFS  $\chi$  spectra for Cu-clay samples treated at pH 4.7 and 7.0 respectively (light lines) compared with the theoretical signals (bold lines). Lower panel: phase shifted Fourier transforms of the experimental data (light lines) and the theoretical signals (bold lines).

where  represents surfaces of the clay minerals with surface hydroxyl groups.

### 3.2. Copper(II) treated clay samples

The EXAFS spectrum of the copper(II) treated clays at low pH (Fig. 2) is consistent with an octahedral oxygen shell with Jahn–Teller distortion. The equatorial Cu–O bond is 1.95 Å whereas the two axial Cu–O bond lengths are 2.30 and 2.65 Å. The goodness of fit parameters improve significantly after adding a Cu–P distance of 3.29 Å (Table 1). However, at neutral pH the main precipitation product on the clay surfaces seems to be copper(I) oxide. The EXAFS spectra recorded at pH 4.7 and 7.0 are almost identical, showing that the speciation is the same at both pH values. The interaction process could be presented as shown in Scheme 2.



Scheme 2.

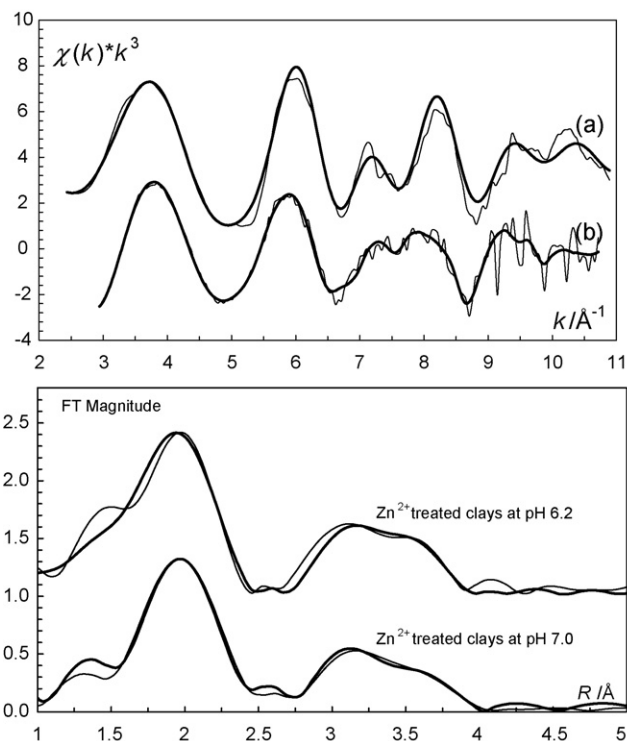
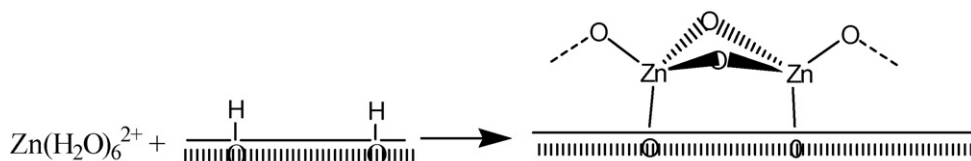


Fig. 3. Upper panel (a) and (b):  $k^3$ -weighted Zn K-edge EXAFS  $\chi$  spectra for Zn-clay samples treated at pH 6.2 and 7.0 respectively (light lines) compared with the theoretical signals (bold lines). Lower panel: phase shifted Fourier transforms of the experimental data (light lines) and the theoretical signals (bold lines).

### 3.3. Zinc(II) treated clay samples

The zinc(II) treated clay samples, adjusted to pH 6.3 and 7.0, shows as the chromium(III) treated ones, a non-sinusoidal shape of the EXAFS functions, Fig. 3. The FT shows light back-scatterer, certainly oxygen, at short distance, 2.0 Å, and a heavier back-scatterer, most probably zinc, at ca. 3.1 Å. Curve-fitting gave Zn–O and Zn···Zn distances of 2.01 and 3.11 Å, respectively. This Zn–O bond distance corresponds to a tetrahedral configuration around zinc, which is significantly shorter than 2.08 Å of the octahedrally hydrated zinc(II) ion. The Zn–O and Zn···Zn distances give a Zn–O–Zn bond angle of 101° suggesting that the ZnO<sub>4</sub> tetrahedra share edges in some kind of polymeric structure. This shows that the zinc(II) ion both hydrolyse, change configuration and polymerise when precipitating on the alkaline clay surface. A similar observation had been



Scheme 3.

$pK_a \approx 9.5$  (depending on temperature and ionic strength), is very close to the  $pH_{PZC}$  of the clay ( $pH_{PZC} = 9.63$ ). However, any precipitation of cadmium(II) oxide or any other cadmium compound with well-defined Cd···Cd distances are not present on the clay surfaces after cadmium treatment. The refined structure parameters are given in Table 1, and the fit of the experimental EXAFS data, and the corresponding FTs, are given in Fig. 4. The cadmium(II) cation may be existing on the surface as presented in Scheme 4.

### 3.5. Mercury(II) treated clay samples

The EXAFS spectrum for the mercury(II) treated clay at low pH (pH 2.2) is dominated by a shell of light-back-scatterer (oxygens) around mercury at very short bond length, 2.00(1) Å, and another shell of heavy back-scatterer at 2.51(1) Å. The distance at 2.51 Å is consistent with Hg–Hg bond of solvated mercury(I) ion,  $Hg_2^{2+}$ , in water, methanol and dimethylsulfoxide [30]. This indicates that the mercury(II) at low pH is reduced to mercury(I) and hydrolysed into almost linear O–Hg–Hg–OH<sub>x</sub> entity,  $x = 1$  or 2, on the surface of the clays. The refined structure parameters are given in Table 1, and the fit of the experimental EXAFS data, and the corresponding FTs, for the low pH mercury(II) sample, are given in Fig. 5. Fig. 6 shows the X-ray absorption near edge structure (XANES) region of the mercury adsorbed on the clays at pH 7.0 and 2.2. There is an expected shift in the absorption energy of 1–2 eV between mercury(I) and mercury(II) which is indicative of the existence of mercury(I) at the low pH and mercury(II) at the neutral pH. The peak on the edge (Fig. 6) is very typical for linear configuration for both mercury(I) and mercury(II) while it is absent when the coordination number is four or higher. For comparison purposes XANES spectrum of the mercury(II) triflate [ $Hg(OH_2)_2(CF_3SO_3)_2$ ] which has a chain structure with the bonds to the water molecules very tightly bound in linear fashion at 2.11 Å and four weak bonds to triflate oxygens at about 2.6 Å, has been added in Fig. 6. The mercury(II) triflate spectrum is similar to the mercury(II) adsorbed clay at pH 7.0. At pH 7.0 only one shell of light back-scatterer around mercury at short bond distance, 2.05(1) Å, is observed in the FT, Fig. 5. This shows that mercury(II) at this pH binds to oxygens in a linear fashion as pre-

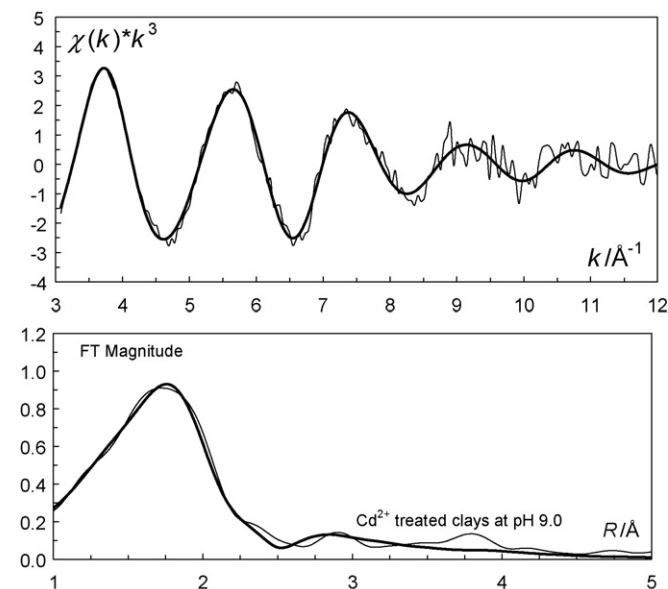
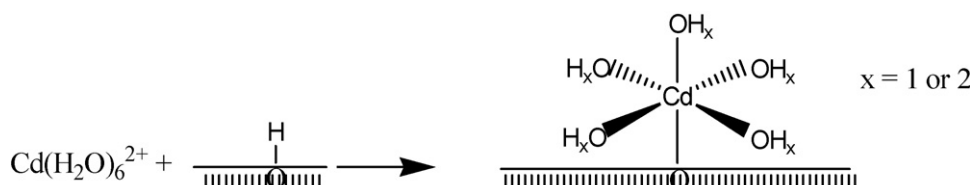


Fig. 4. Upper panel:  $k^3$ -weighted Cd K-edge EXAFS  $\chi$  spectra for Cd-clay samples treated at pH 9 (light line) compared with the theoretical signal (bold line). Lower panel: non-phase shifted Fourier transforms of the experimental data (light line) and the theoretical signal (bold line).

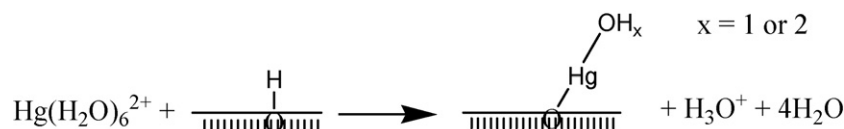
made on adsorption of Zn on hydroxyapatite surface [16] with Zn–O, Zn···Zn and Zn···Zn distances of 1.99, 3.11 and 3.60 Å, respectively, though it was not possible to determine the compound containing these Zn···Zn distances and many alternatives such as hydrozincate may be suggested. Based on this study the zinc(II) species on the surface can be presented as in Scheme 3.

### 3.4. Cadmium treated clay sample

The Fourier transform (FT) of the cadmium treated clay sample shows a single Cd–O distance at 2.27 Å, and weak multiple scattering at the double bond distance, Fig. 4, which corresponds to an octahedral  $CdO_6$  complex [29]. Whether cadmium is sorbed to the clay surface as the hydrated ion or if it is hydrolysed is not possible to evaluate from the EXAFS data since the hydrolysis constant of cadmium(II) in aqueous solution,



Scheme 4.



Scheme 5.

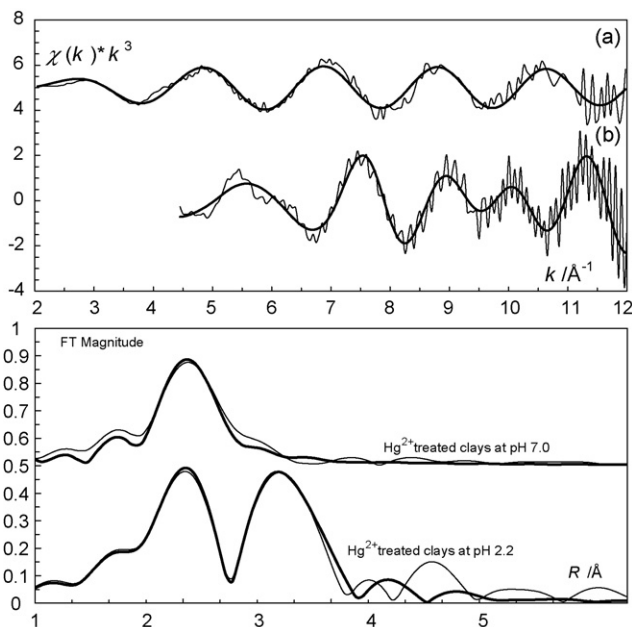


Fig. 5. Upper panel (a) and (b):  $k^3$ -weighted Hg L<sub>III</sub>-edge EXAFS  $\chi$  spectra for Hg-clay samples at pH 7.0 and 2.2 respectively (light lines) compared with the theoretical signals (bold lines). Lower panel: phase shifted Fourier transforms of the experimental data (light lines) and the theoretical signals (bold lines).

viously found for adsorbed mercury(II) ion on goethite surfaces [13] and in solid mercury(II) oxide and bisaquamercury(II) trifluoromethanesulfonate. It seems very likely that the mercury(II) is sorbed to the clay surface as a hydrolysis complex. Since hydrated mercury(II) ions easily hydrolyse ( $pK_a \approx 3.5$  depending on temperature and ionic strength) and that no Hg $\cdots$ Hg distances (pH 7) are observed, no precipitation of HgO occurs.

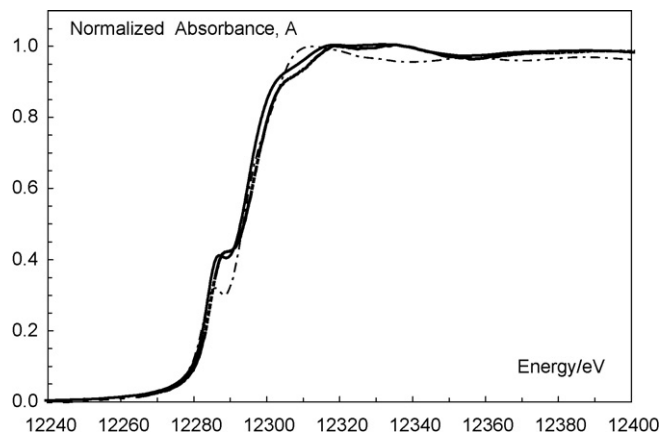
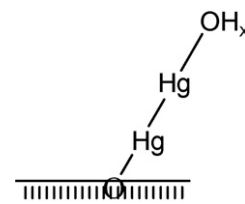


Fig. 6. XANES spectra of the mercury adsorbed clays at pH 7.0 (heavy dotted spectrum), pH 2.2 (heavy dark spectrum) and mercury(II) triflate (light dotted spectrum).



Scheme 6.

The refined structure parameters are given in Table 1. The proposed structure of the Hg(II) species on the clay surface is given in Scheme 5.

At low pH the linear hydrolysed mercury(I) could structurally be presented as shown in Scheme 6.

### 3.6. Lead(II) treated clay samples

The adsorption studies of lead(II) on the clays showed that lead(II) is strongly adsorbed above pH 7 [10]. This is supported in this study by the large edge step observed in the EXAFS spectrum of the lead(II) treated clay samples (Fig. 7). However, the EXAFS features are very weak showing that the lead does not have any well-defined structure on the surfaces. It is common that the structures of lead(II) have very low symmetry, due to the lone  $6s^2$  electron-pair, and that a wide range of coordination numbers have been reported [31–33]. The absence of a well-defined EXAFS function in spite of large amounts of lead(II), seen by the large edge step, can be explained by the presence of several lead(II) compounds with varying structure and configuration around lead(II). This causes the distribution of Pb–O bond distances to become very large, and thereby hardly observable by EXAFS. Hydrolysis of lead(II) salts at very high concentra-

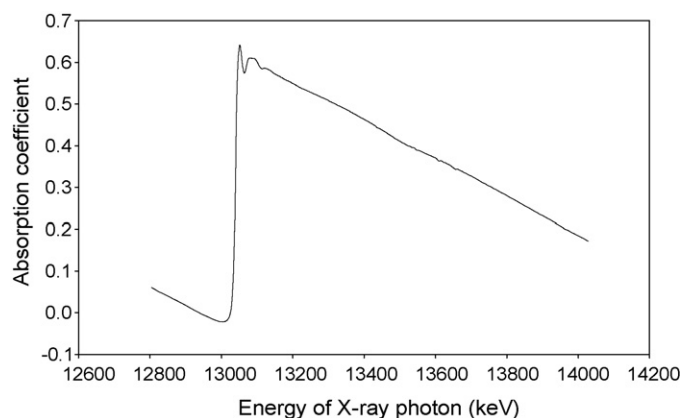


Fig. 7. Absorption coefficient as a function of energy for the Pb L<sub>III</sub>-edge of the Pb-clay samples at neutral pH.

tion result in tetranuclear and hexanuclear species  $[\text{Pb}_4(\text{OH})_4^{4+}]$  and  $[\text{Pb}_6(\text{OH})_8^{4+}]$  as the predominant species [31]. However, these types of hydrolysis products should easily be detected by EXAFS as they contain defined Pb–Pb distances [34].

#### 4. Discussion

Clays are hydrous aluminium silicates which are classified as either 1:1 or 2:1 clay minerals. The sheets in these clays are held together by weak van de Waals forces making it easy for other chemicals to enter the interlayer region. There are three types of crystalline surfaces onto which metal adsorption can occur on the clays: a hydroxyl plane associated with the alumina octahedral layer, an oxygen plane on the silica tetrahedral layer and particle edges formed from the incomplete or irregular lattice structure. Many 2:1 clay minerals have permanent negative charge due to isomorphous substitution of aluminium(III) for silicon(IV) in the silica layer or magnesium(II) for aluminium(III) in the alumina layer [35]. The Tundulu natural clays used in this study have high  $\text{pH}_{\text{PZC}}$  of 9.63, indicating that the surfaces are highly alkaline, and this influences metal hydrolysis and precipitation as additional metal sorption mechanisms. The pH dependence of the sorption of chromium(III), copper(II), zinc(II), cadmium(II), mercury(II) and lead(II) on these clays have been discussed in a previous paper [10]. With the heterogeneous nature of the clays it is likely that several metal sorption mechanisms take place simultaneously making the determination of metal/clay component interaction difficult on such material. However, this EXAFS study has shown that the high alkalinity of the clay promotes hydrolysis of heavy metals which then precipitate and get sorbed on the surface. In all cases it was shown that oxygen atoms occupy the first shells of the metal atoms on the surface.

The hydrated chromium(III) ion hydrolyses largely into  $[\text{Cr}_3(\text{OH})_4(\text{H}_2\text{O})_{10}]^{5+}$  at low pH indefinite  $[\text{Cr}(\text{OH})_x(\text{OH})_2]_n^{n(2x-3)+}$  chains are formed at high pH values. These polymeric hydrolysis complexes present in the aqueous phase are adsorbed and/or precipitate out onto the clay surfaces.

Copper(II) treated clays EXAFS analysis indicates an octahedral first shell of oxygen atoms with Jahn–Teller distortion and Cu–P average bond length of 3.12 Å. The corresponding 3-leg Cu–O–P scattering distance of 3.23 Å was also obtained. These results suggest that the copper(II) is sorbed to the clay mixture preferably through the phosphate groups of the non-clay component of the mixture, fluoroapatite.

Zinc(II) hydrolyzes sparingly in acidic media to produce  $\text{ZnOH}^+$  and  $\text{Zn}_2\text{OH}^{3+}$  before precipitation commences in the neutral region while  $\text{Zn}(\text{OH})_4^{2-}$  and  $\text{Zn}_2(\text{OH})_6^{2-}$  are formed in the alkaline media [31]. In this work, polymeric  $\text{ZnO}_4$  edge sharing tetrahedral species are present on the clay surfaces suggesting that precipitation is the mechanism through which zinc(II) species are sorbed and hydrolysed on the alkaline clay surfaces.

This EXAFS study showed that the cadmium(II) is sorbed on the alkaline clay surfaces as mononuclear species with octahedral  $\text{CdO}_6$  configuration. However, it is hard to judge

whether the cadmium(II) ion is sorbed to the clay surface as the hydrated ion or if it is partly hydrolysed based on the EXAFS data.

#### 5. Conclusions

Chromium(III), copper(II), zinc(II), cadmium(II), mercury(II) and lead(II) sorbed on natural alkaline mixed clays were studied using EXAFS spectroscopy. Chromium(III) and zinc(II) are sorbed as hydrolysed octahedral and tetrahedral polynuclear complexes, respectively. Copper(II) is mainly sorbed through the phosphate groups of the fluoroapatite in the adsorbent mixture. Mercury(II) is adsorbed as hydrolysed linear O–Hg–O units on the clay surface at neutral pH, while it is reduced to mercury(I) at low pH and adsorbed as  $\equiv\text{O–Hg–Hg–OH}_x$  complexes ( $x = 1$  or 2). Cadmium(II) binds six oxygens in a regular octahedral fashion but it is not possible to distinguish whether it is hydrated or partly hydrolysed. No precise chemical environment around the lead(II) could be obtained for the lead(II) treated clays. This work therefore suggests that hydrolysis and precipitation govern uptake of the studied heavy metal ions by this kind of natural alkaline mixed clay.

#### Acknowledgements

We would like to thank the International Science Program (ISP) through the International Program in Chemical Sciences (IPICS) at Uppsala University for granting financial assistance for this ongoing work on water quality and pollution control in Malawi, and for providing a fellowship for S. Sajidu to study in the University of Malawi and also do some experimental work at the Swedish University of Agricultural Sciences within the Malawi MAW:02 project. The Geological Survey of Malawi is also acknowledged for providing the clay material. We are also grateful to MAX-lab, Lund University, for the allocation of beam time and laboratory facilities. MAX-lab is supported by the Swedish Research Council and the Knut and Alice Wallenberg Foundation, with additional support from the Crafoord Foundation and the Faculty of Science and Technology, Nowergian University of Science and Technology.

#### References

- [1] M.F. Brigatti, F. Corradini, G.C. Franchini, S. Mazzoni, L. Medici, L. Poppi, Interaction between montmorillonite and pollutants from industrial wastewaters: exchange of  $\text{Zn}^{2+}$  and  $\text{Pb}^{2+}$  from aqueous solutions, *Appl. Clay Sci.* 9 (1995) 383–395.
- [2] M.F. Brigatti, S. Colonna, D. Malferrari, L. Medici, L. Poppi, Mercury adsorption by montmorillonite and vermiculite: a combined XRD, TG-MS, and EXAFS study, *Appl. Clay Sci.* 28 (2005) 1–8.
- [3] D. Malferrari, M.F. Brigatti, A. Laurora, S. Pini, L. Medici, Sorption kinetics and chemical forms of Cd(II) sorbed by thiol-functionalised 2:1 clay minerals, *J. Hazard. Mater.* 143 (2007) 73–81.
- [4] K. Okada, K. Nishimuta, Y. Kameshima, A. Nakajima, Effect on uptake of heavy metal ions by phosphate grafting of allophane, *J. Colloid Interf. Sci.* 286 (2005) 447–454.
- [5] P. Srivastava, B. Singh, M. Angove, Competitive adsorption behaviour of heavy metals on kaolinite, *J. Colloid Interf. Sci.* 290 (2005) 28–38.



- [6] R. Donat, A. Akdogan, E. Erdem, H. Cetisli, Thermodynamics of  $\text{Pb}^{2+}$  and  $\text{Ni}^{2+}$  adsorption onto natural bentonite from aqueous solutions, *J. Colloid Interf. Sci.* 286 (2005) 43–52.
- [7] S. Veli, B. Alyüz, Adsorption of copper and zinc from aqueous solutions by using natural clay, *J. Hazard. Mater.* 149 (2007) 226–233.
- [8] E.J. Elzinga, D.L. Sparks, Reaction condition effects on Nickel sorption mechanism in illite-suspension, *Soil Sci. Soc. Am. J.* 65 (2001) 94–101.
- [9] L.M. Mataka, E.M.T. Henry, W.R.L. Masamba, S.M.I. Sajidu, Lead remediation of contaminated water using *Moringa Stenopetala* and *Moringa oleifera* seed powder, *Int. J. Environ. Sci. Technol.* 3 (2) (2006) 131–139.
- [10] S.M.I. Sajidu, I. Persson, W.R.L. Masamba, E.M.T. Henry, D. Kayambazinthu, Removal of  $\text{Cd}^{2+}$ ,  $\text{Cr}^{3+}$ ,  $\text{Cu}^{2+}$ ,  $\text{Hg}^{2+}$ ,  $\text{Pb}^{2+}$  and  $\text{Zn}^{2+}$  cations and  $\text{AsO}_4^{3-}$  anions from aqueous solutions by mixed clay from Tundulu in Malawi and characterisation of the clay, *Water SA* 32 (4) (2006) 519–526.
- [11] S.M.I. Sajidu, E.M.T. Henry, I. Persson, W.R.L. Masamba, D. Kayambazinthu, pH dependence of sorption of  $\text{Cd}^{2+}$ ,  $\text{Zn}^{2+}$ ,  $\text{Cu}^{2+}$ , and  $\text{Cr}^{3+}$ , on crude water and sodium chloride extracts of *Moringa stenopetala* and *Moringa oleifera*, *Afr. J. Biotechnol.* 5 (23) (2006) 2397–2401.
- [12] R. Takamatsu, K. Asakura, W. Chun, T. Miyazaki, M. Nakano, EXAFS studies about sorption of cadmium ions on montmorillonite, *Chem. Lett.* 35 (2) (2006) 224–225.
- [13] C.R. Collins, D.M. Sherman, K.V. Ragnarsdottir, Surface complexation of  $\text{Hg}^{2+}$  on goethite: mechanism from EXAFS spectroscopy and density functional calculations, *J. Colloid Interf. Sci.* 219 (1999) 345–350.
- [14] C.S. Kim, J.J. Rytuba, G.E. Brown Jr., EXAFS study of mercury(II) sorption to Fe- and Al-(hydr)oxides: effects of chloride and sulfate, *J. Colloid Interf. Sci.* 270 (2004) 9–20.
- [15] S.E. Fendorf, G.M. Lamble, M.G. Stepleton, M.J. Kelly, D.L. Sparks, Mechanisms of chromium(III) sorption on silica. 1. Cr(III) surface structure derived by extended X-ray absorption fine spectroscopy, *Environ. Sci. Technol.* 28 (1994) 284–289.
- [16] Y.J. Lee, E.J. Elzinga, R.J. Reeder, Sorption mechanisms of zinc on hydroxyapatite: systematic uptake studies and EXAFS spectroscopy analysis, *Environ. Sci. Technol.* 39 (2005) 4042–4048.
- [17] G.W. Kunze, J.B. Dixon, Pretreatment for mineralogical analysis, in: A. Klute (Ed.), *Methods of Soil Analysis. Part 1. Physical and Mineralogical Methods*, 2nd edition, ASA and SSSA, Madison, WI, 1986, pp. 99–100.
- [18] L. Ammann, Cation Exchange and Adsorption on Clays and Clay Minerals, Ph.D. Thesis, Christian-Albrecht Universität, Kiel, Germany, 2003.
- [19] A. Thompson, D. Attwood, E. Gullikson, M. Howells, K.J. Kim, J. Kirz, J. Kortright, I. Lindau, P. Pianatta, A. Robinson, J. Scofield, J. Underwood, D. Vaughan, G. Williams, H. Winick, X-ray Data Booklet, LBNL/PUB-490 Rev. 2, Lawrence Berkeley National Laboratory, Berkeley, CA, 2001.
- [20] G.N. George, I.J. Pickering, EXAFSPAK—A Suite of Computer Programs for EXAFS Analysis, SSRL, Stanford University, CA, USA, 1993.
- [21] (a) FEFF code for ab initio calculations of XAFS: J.M. de Leon, J.J. Rehr, S.I. Zabinsky, R.C. Albers, *Phys. Rev. B* 44 (1991) 4146;
- (b) S.I. Zabinsky, J.J. Rehr, A.L. Ankudinov, R.C. Albers, M.J. Eller, *Phys. Rev. B* 52 (1995) 2995;
- (c) A.L. Ankudinov, Ph.D Thesis, University of Washington, Seattle, USA, 1996.
- [22] G. Johansson, M. Sandström, The crystal structure of hexaqua-cadmium(II) perchlorate,  $[\text{Cd}(\text{H}_2\text{O})_6](\text{ClO}_4)_2$ , *Acta Chem. Scand. Ser. A* 41 (1987) 113–116.
- [23] R.E. Marsh, H. Herstein, Some additional changes in space groups of published crystal structures, *Acta Crystallogr. Sect. B* 39 (1983) 280–287;
- W. Massa, Wasserstoffbrücken in fluoridhaltigen Festkörpern. I. Darstellung, Eigenschaften und Kristallstruktur von  $(\text{NH}_4)_2[\text{Cr}(\text{H}_2\text{O})_6]\text{F}_5$ , *Z. Anorg. Allg. Chem.* 52 (1995) 2995.
- [24] V.A. Voronin, V.V. Shchennikov, Change of structure of mercury oxide under the action of pressure, *Kristallografiya* 34 (1989) 491–493.
- [25] A. Molla-Abbassi, L. Eriksson, J. Mink, I. Persson, M. Sandström, M. Skripkin, A.S. Ullström, P. Lindqvist-Reis, Structure and bonding of bisaquamercury(II) and trisaquathallium(III) trifluoromethanesulfonate., *J. Chem. Soc., Dalton Trans.* (2002) 4357–4364.
- [26] R. Stahl, H. Jacobs, Zur Kristallstruktur von  $\text{Sr}[\text{Zn}(\text{OH})_4]\cdot\text{H}_2\text{O}$ , *Z. Anorg. Allg. Chem.* 623 (1997) 1273–1276.
- [27] J. Albertsson, S.C. Abrahams, Å. Kvik, Atomic displacement, anharmonic thermal vibration, expansivity and pyroelectric coefficient thermal dependences in  $\text{ZnO}$ , *Acta Crystallogr. Sect. B* 45 (1989) 34–40.
- [28] N. Torapava, D. Davydov, I. Persson, Hydration and hydrolysis of chromium(III) in aqueous solution, unpublished results.
- [29] P. D'Angelo, G. Chillemi, V. Barone, G. Mancini, N. Sanna, I. Persson, Experimental evidence for a variable first coordination shell of the Cadmium (II) ion in aqueous, dimethyl sulfoxide, and *N,N'*-dimethylpropyleneurea solution, *J. Phys. Chem. B* 109 (2005) 9178–9185.
- [30] J. Rosdahl, I. Persson, L. Kloo, K. Ståhl, On the salvation of the mercury(I) ion. A structural spectroscopic and quantum chemical study, *Inorg. Chim. Acta* 357 (2004) 2624–2634.
- [31] C.F. Baes Jr., R.E. Mesmer, *The Hydrolysis of Cations*, Reprint edition, Krieger Publishing Company, Malabar, FL, 1986.
- [32] F.H. Allen, S. Bellard, M.D. Brice, B.A. Cartwright, A. Doubleday, H. Higgs, T. Hummelink, C.G. Hummelink-Peters, O. Kennard, W.D.S. Motherwell, J.R. Rodgers, D.G. Watson, *The Cambridge Crystallographic Data Centre: computer based search, retrieval, analysis and display of information*, *Acta Crystallogr. Sect. B* 35 (1979) 2331.
- [33] *Inorganic Crystal Structure Data Base*, National Institute of Standards and Technology, Fachinformationszentrum, Karlsruhe, Release 07/2.
- [34] G. Johansson, A. Olin, On the structure of the dominating hydrolysis products of lead(II) in solution, *Acta Chem. Scand.* (1968) 3197–3201.
- [35] J.P. Gustafsson, G. Jacks, M. Simonsson, I. Nilsson, *Soil and Water Chemistry*. Lantbruks Universitet Sveriges (SLU), KTH Arkitektur och samhällsbyggnad, Uppsala, Sweden, 2005.